Electronic Supplementary Material

Creating magnetic ionic liquid molecularly imprinted polymers for selective extraction of lysozyme

Wei Xu[a], Qingzhou Dai[a],Yuzhi Wang[a]*, Xiaojian Hu[b]*, Panli Xu[a], Rui Ni[a], Jiaojiao Meng[a]

[a] State Key Laboratory of Chemo/Biosensing and Chemometrics, College of Chemistry and Chemical Engineering, Hunan University, Changsha, 410082, P.R. China

[b] Department of Chemistry, School of Basic Medicine, Changsha Medical University, Changsha, 410219, P.R. China

Corresponding author: Professor Yuzhi Wang; Associate professor Xiaojian Hu

State Key Laboratory of Chemo/Biosensing and Chemometrics

College of Chemistry and Chemical Engineering

Hunan University

Changsha 410082

P. R. China

Phone: +86-731-88821903

Fax: +86-731-88821848

E-mail: wyzss@hnu.edu.cn

Table S1 Preparative composition of different MIPs.

MIPs (mg)	Fe_3O_4@VTEO (mg)	IL (mg)	Lys (mg)	MBAA (mg)	20%APS (μL)	20%TEMED (μL)
MIP1	100	100	25	20	75	75
MIP2	100	150	25	20	75	75
MIP3	100	200	25	20	75	75
MIP4	100	250	25	20	75	75
MIP5	100	300	25	20	75	75
NIP1	100	100	-	20	75	75
NIP2	100	150	-	20	75	75
NIP3	100	200	-	20	75	75
NIP4	100	250	-	20	75	75
NIP5	100	300	-	20	75	75

Table S2 Langmuir isotherm constants of the magnetic materials.

Magnetic materials	**[a]K_L (mL·mg^{-1})**	**[b]Q_{max} (mg·g^{-1})**	**R^2**
Fe_3O_4@VTEO@IL-MIPs	116	213	0.9985
Fe_3O_4@VTEO@IL-NIPs	299	121	0.9993

Where [a]K_L is the equilibrium constant of Langmuir adsorption, [b]Q_{max} is the theoretical maximum adsorption capacity.

Characterization of Fe_3O_4@VTEO@IL-MIPs

The FT-IR spectra of [AAPIM]Cl, Fe_3O_4, Fe_3O_4@VTEO, Fe_3O_4@VTEO@IL-NIPs and Fe_3O_4@VTEO@IL-MIPs were illustrated in Fig. S1. The characteristic peak at 573 cm^{-1} (Fig. S1) is assigned to the stretching vibration of Fe-O.[1] The spectrum of Fe_3O_4@VTEO in Fig. S1b contains peaks at 1653 and 1130 cm^{-1} corresponding to C=C stretching vibration and Si-O-Si asymmetric stretching vibration, respectively. The phenomenon indicates that the successful modification of VTEO.[2] In the spectrum of Fe_3O_4@VTEO@IL-NIPs (Fig. S1d), the characteristic peaks of polymer layer are not clearly observed. However, double peaks of amino group at 3400-3100 cm^{-1} are observed in Fe_3O_4@VTEO@IL-MIPs (stretching vibrations of N-H) (Fig. S1c), which confirms the presence of the NH-IL monomer and the successful modification of polymer layer. In the spectrum of [AAPIM]Cl (Fig. S1e), the stretching vibrations of N-H at 3430 and 3365 cm^{-1} are presented. Moreover, the characteristic bands of C=C are observed at 1680 and 1630 cm^{-1}, and the characteristic signals of imidazolium C=N stretching vibration are observed at 1570 and 1454 cm^{-1}, which indicates the successful synthesis of IL.

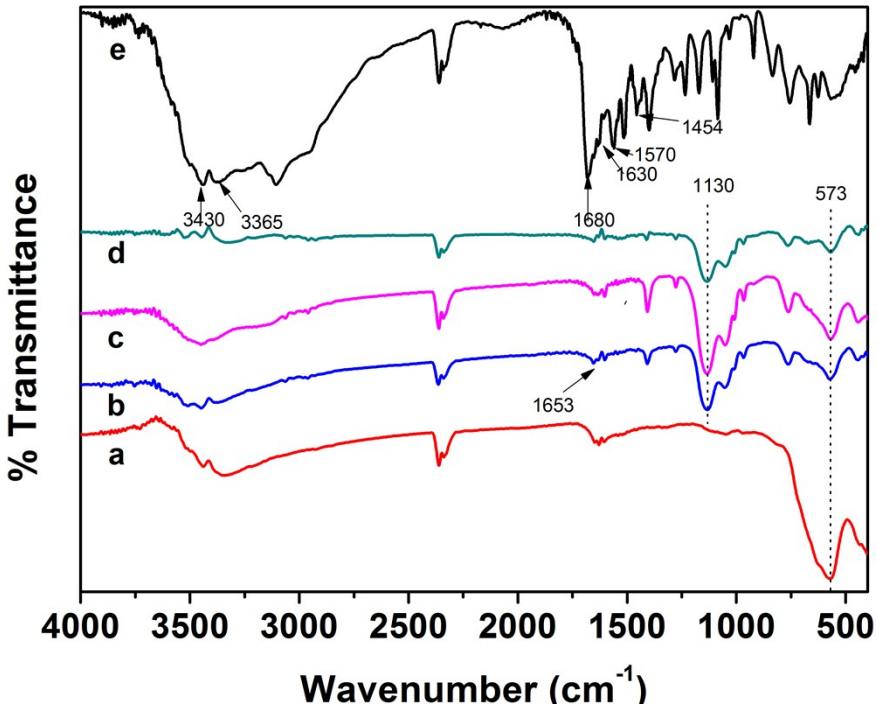

Fig. S1 The FT-IR spectra of Fe_3O_4 (a), Fe_3O_4@VTEO (b), Fe_3O_4@VTEO@IL-MIPs (c), Fe_3O_4@VTEO@IL-NIPs (d) and [AAPIM]Cl (e).

The sizes and morphologies of Fe_3O_4, Fe_3O_4@VTEO and Fe_3O_4@VTEO@IL-MIPs were determined by TEM which was shown in Fig. S2. The average diameter of Fe_3O_4 is in the range of 10-20 nm (Fig. S2a). It is clear that the Fe_3O_4 nanoparticles conglomerated seriously. After coating with VTEO, the diameter of Fe_3O_4@VTEO particles is higher than Fe_3O_4 nanoparticles obviously (Fig. S2b). It can be seen from Fig. S2c that a gray shell is observed on the surface of the Fe_3O_4@VTEO particles, which offers strong evidence of the successful formation of IL imprinting layer.

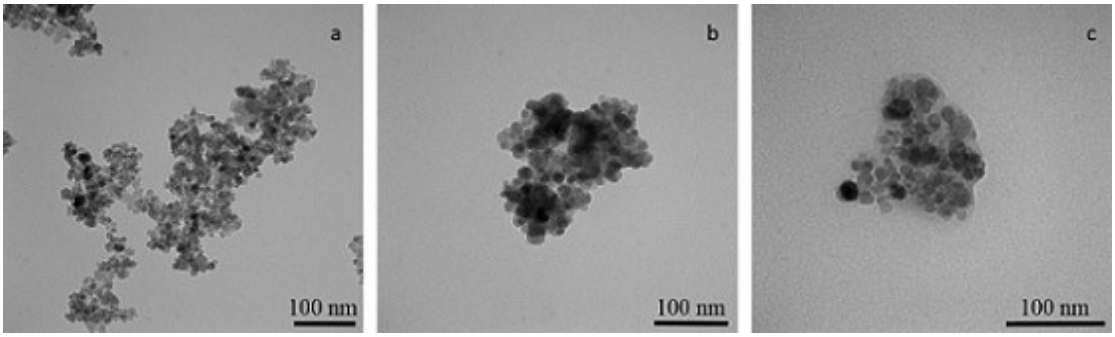

Fig. S2 The TEM images of Fe_3O_4 (a), Fe_3O_4@VTEO (b) and Fe_3O_4@VTEO@IL-MIPs (c).

The particles size were measured by dynamic light scattering (DLS) study (Fig. S3). Compared with TEM pictures, the measurements of the size obtained were bigger, which could be explicated by agglomeration of the particles in aqueous solution and the hydratization of particles. It is clear that the VTEO layer and the MIPs layer make the particle size bigger than Fe_3O_4. However, some particles agglomerated after coating with VTEO and MIPs layer also. This is beacause some Fe_3O_4 particles may be crosslinked by VTEO or MIPs, even Fe_3O_4@VTEO and Fe_3O_4@VTEO@IL-MIPs particles may agglomerate in aqueous.

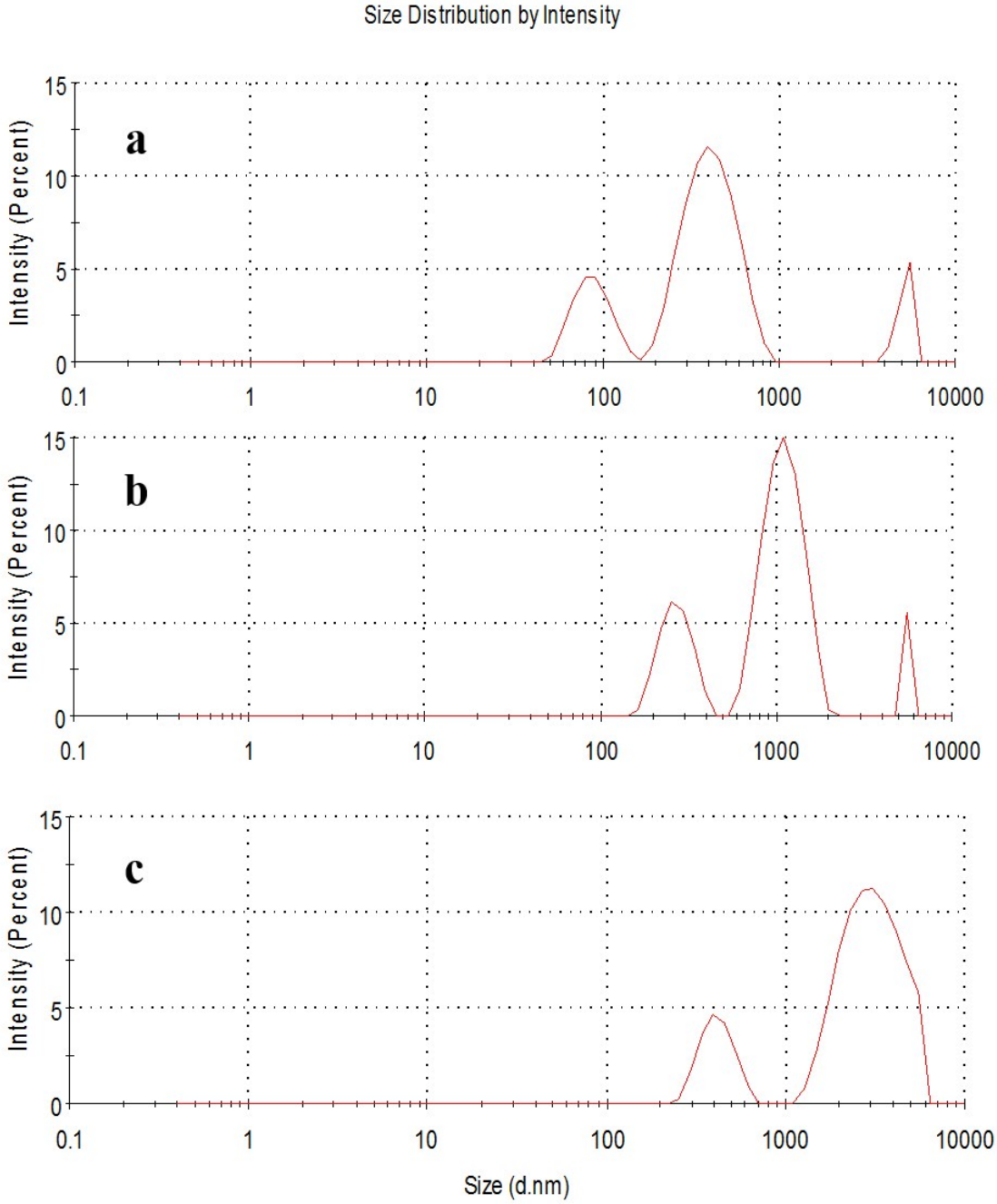

Fig. S3 DLS analysis of Fe_3O_4(a), Fe_3O_4@VTEO(b) and Fe_3O_4@VTEO@IL-MIPs (c).

The magnetic properties of Fe_3O_4, Fe_3O_4@VTEO and Fe_3O_4@VTEO@IL-MIPs were evaluated by VSM, and the magnetic hysteresis curves were shown in Fig. S4A. The saturation magnetization of Fe_3O_4, Fe_3O_4@VTEO and Fe_3O_4@VTEO@IL-MIPs are 68.56, 42.27 and 39.09 emu/g, respectively. The reducing of saturation magnetization in Fe_3O_4@VTEO and Fe_3O_4@VTEO@IL-MIPs is caused by the successful modification of VTEO and polymer layer. This is consistent with the observation from TGA. As illustrated in Fig. S4B, the MIPs particles can be separated rapidly by a magnet about 6 s, which contributes to the separation of Lys in real sample application.

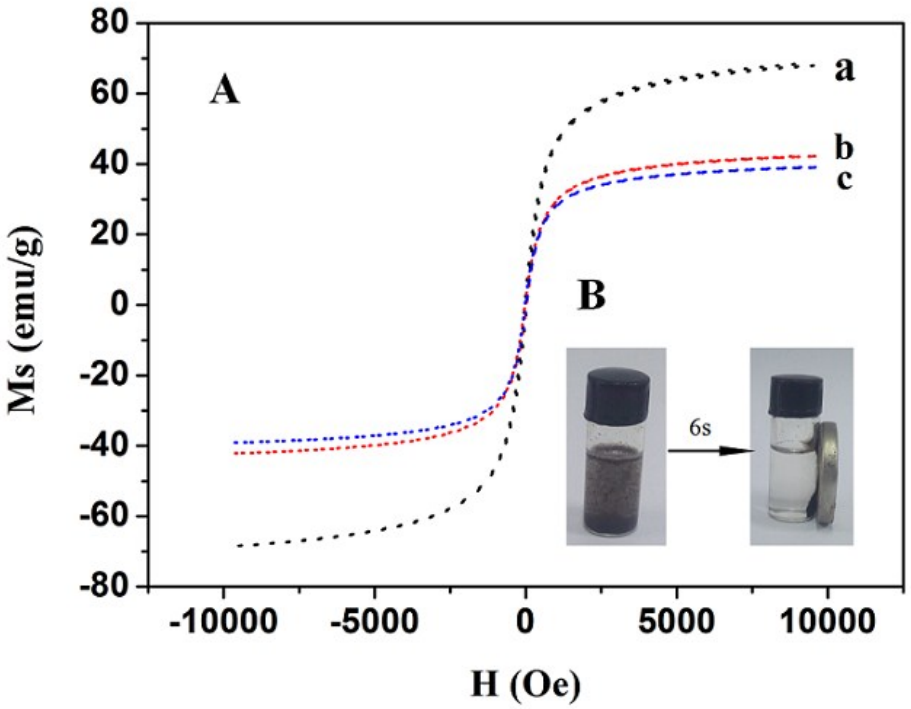

Fig. S4 The magnetic hysteresis loops of Fe_3O_4 (a), Fe_3O_4@VTEO (b) and Fe_3O_4@VTEO@IL-MIPs (c).

The relative composition of Fe_3O_4, Fe_3O_4@VTEO and Fe_3O_4@VTEO@IL-MIPs were characterized by TGA. As displayed in Fig. S5, the weight loss of pure Fe_3O_4 nanoparticles is only 4.6% when the temperature increases to 1000 °C. The Fe_3O_4@VTEO particles presented a weight loss of 0.2% in the temperature range of 0-200 °C, which is the release of water molecules. When the temperature increased to 1000 °C, the other decline in weight (about 18.2%) is resulted from the decomposition of VTEO coated on Fe_3O_4. For Fe_3O_4@VTEO@IL-MIPs, a weight loss of about 1.4% is discovered at 200 °C, which is because the existence of imprinted cavities absorb more water than Fe_3O_4@VTEO. At 200-1000 °C, Others decrease in weight is about 27.9% for the decomposition of MIPs coating, which confirms the formation of the IL polymers layer.

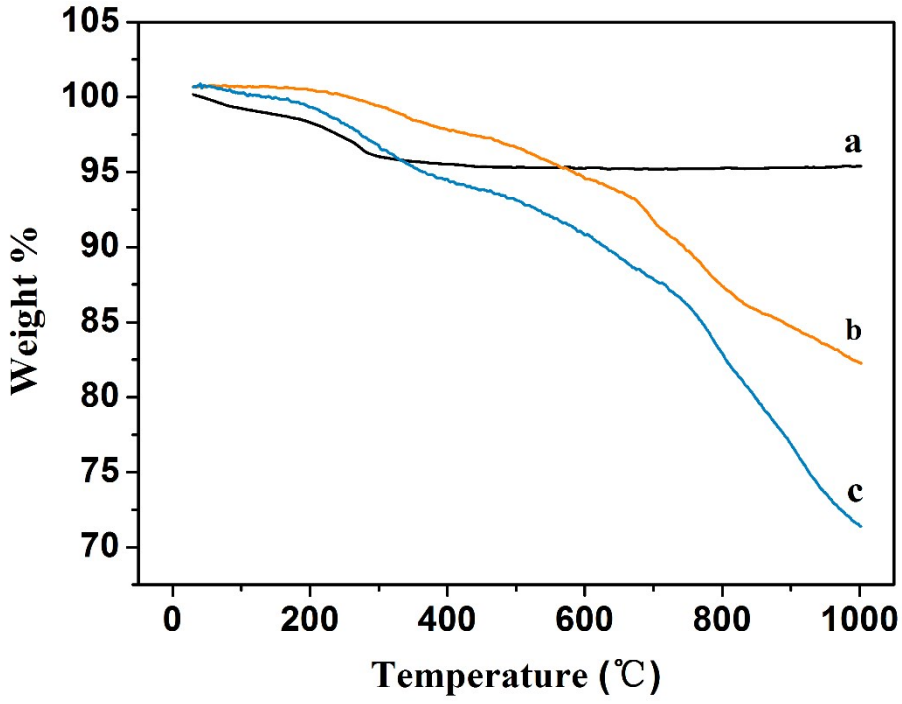

Fig. S5 Weight loss curves of Fe_3O_4 (a), Fe_3O_4@VTEO (b) and Fe_3O_4@VTEO@IL-MIPs (c).

The phases and the structures of Fe_3O_4, Fe_3O_4@VTEO and Fe_3O_4@VTEO@IL-MIPs were investigated by XRD, which were illustrated in Fig. S6. Six characteristic diffraction peaks of Fe_3O_4 can be observed in Fig. S6a, which are assigned to (220), (311), (400), (422), (511) and (440) planes of Fe_3O_4 crystal. According to Fig. S6b-c, the similar diffraction peaks are detected in patterns of Fe_3O_4@VTEO and Fe_3O_4@VTEO@IL-MIPs. Compared with the Fe_3O_4 reflection, there are obvious broad peaks appear from 2θ=20° to 30° (Fig. S6b-c). It is resulted from the amorphous peak of silica. Apparently, XRD patterns provide a strong evidence that microspheres contain Fe_3O_4 with cubic inverse spinel structure and the synthesis processes do not change the phase of Fe_3O_4.

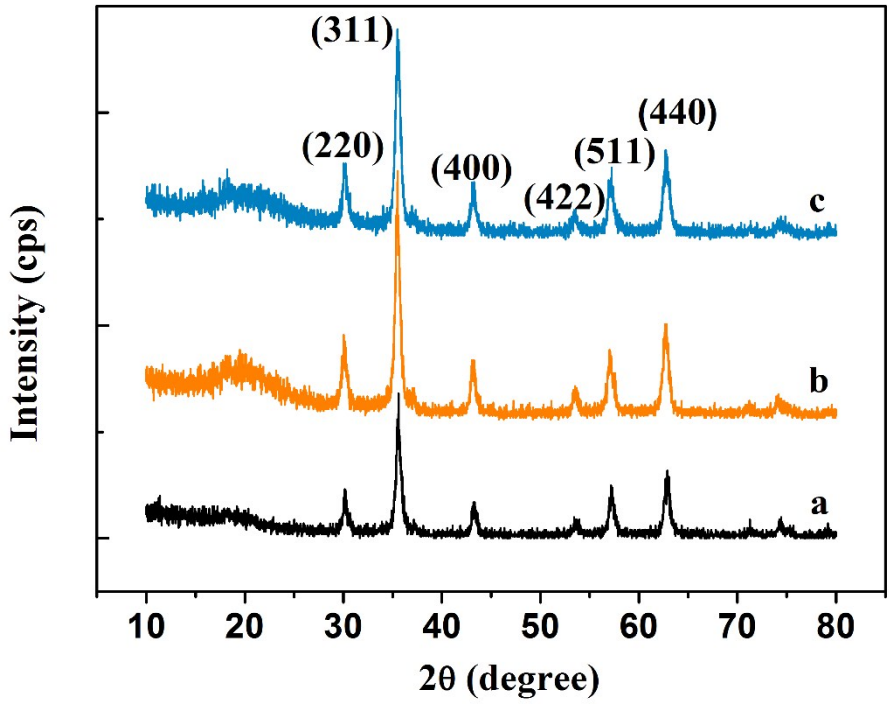

Fig. S6 X-ray diffraction patterns of Fe_3O_4 (a), Fe_3O_4@VTEO (b) and Fe_3O_4@VTEO@IL-MIPs (c).

Adsorption isotherms

$$\frac{C_e}{Q_e} = \frac{1}{Q_{max} K_L} + \frac{C_e}{Q_{max}}$$

Where C_e ($mg \cdot mL^{-1}$) is the concentration of Lys in the final equilibrium solution, Q_e ($mg \cdot g^{-1}$) and Q_{max} ($mg \cdot g^{-1}$) are the experimental adsorption capacity and the theoretical maximum adsorption capacity of Fe_3O_4@VTEO@IL-MIPs (NIPs) for the template protein, respectively. K_L ($mL \cdot mg^{-1}$) is the equilibrium constant of Langmuir adsorption. The linear fitting curves of the Langmuir model were plotted in C_e/Q_e versus C_e, which were shown in Fig. S7 and Table S2. From the linear fitting curves, it can be seen that C_e/Q_e and C_e has a good linear relationship. The R^2 of both Fe_3O_4@VTEO@IL-MIPs and Fe_3O_4@VTEO@IL-NIPs are higher than 0.99, which proves the Langmuir equation fits well for Lys adsorption within the studied concentration range.[3]

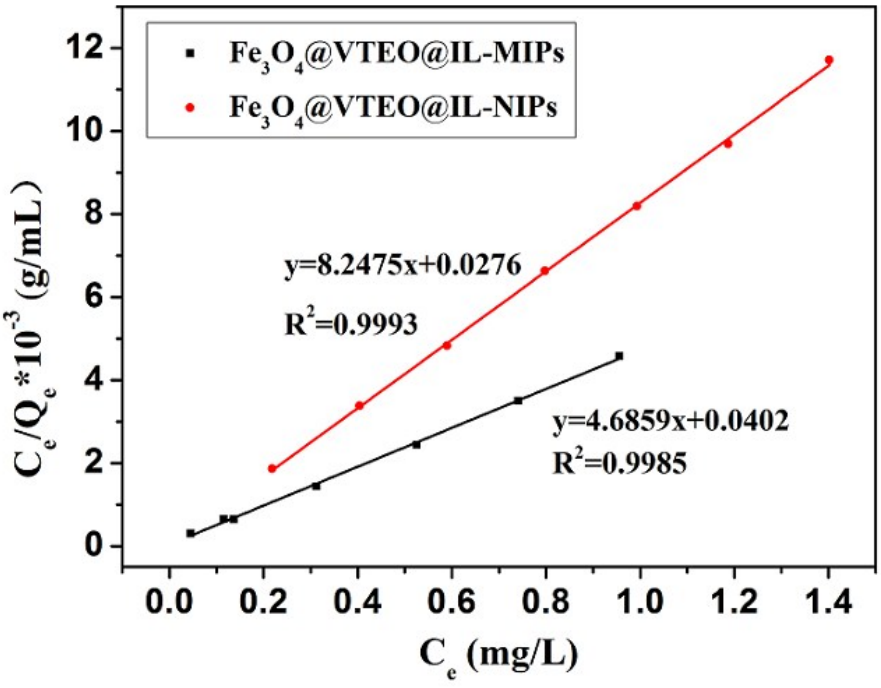

Fig. S7 Langmuir adsorption models of Lys on Fe_3O_4@VTEO@IL-MIPs and Fe_3O_4@VTEO@IL-NIPs.

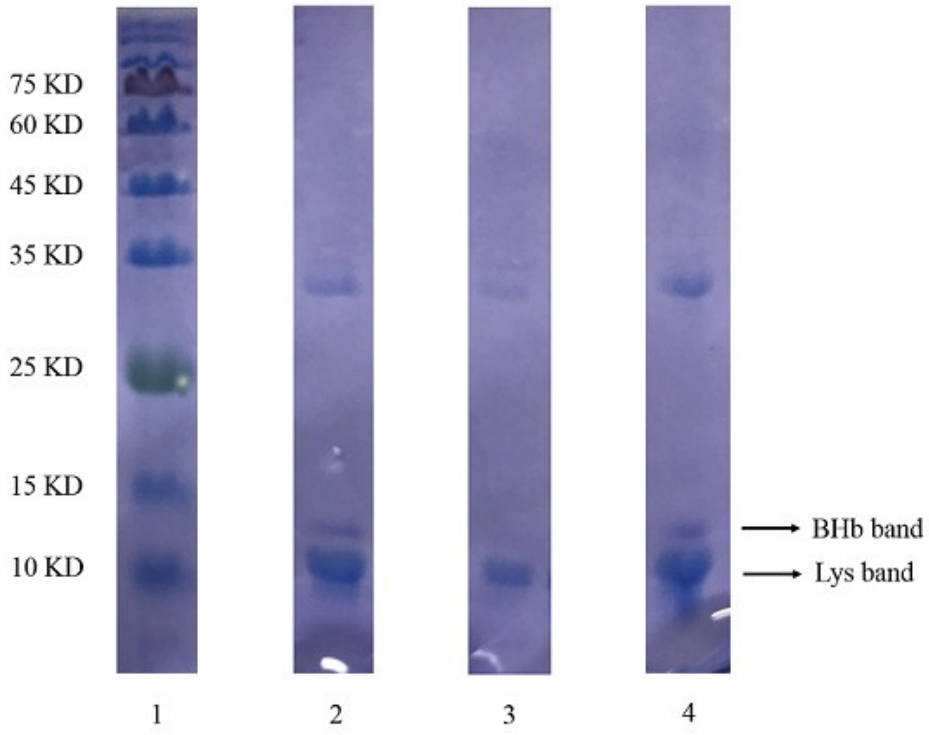

Fig. S8 The results of SDS-PAGE analysis for the purification of Lys from a binary protein mixture. Lane 1, protein molecular weight marker; Lane 2, protein mixture solution after the adsorption by Fe_3O_4@VTEO@IL-NIPs; Lane 3, protein mixture solution after adsorption by Fe_3O_4@VTEO@IL-MIPs; Lane 4, protein mixture solution containing Lys and BHb.

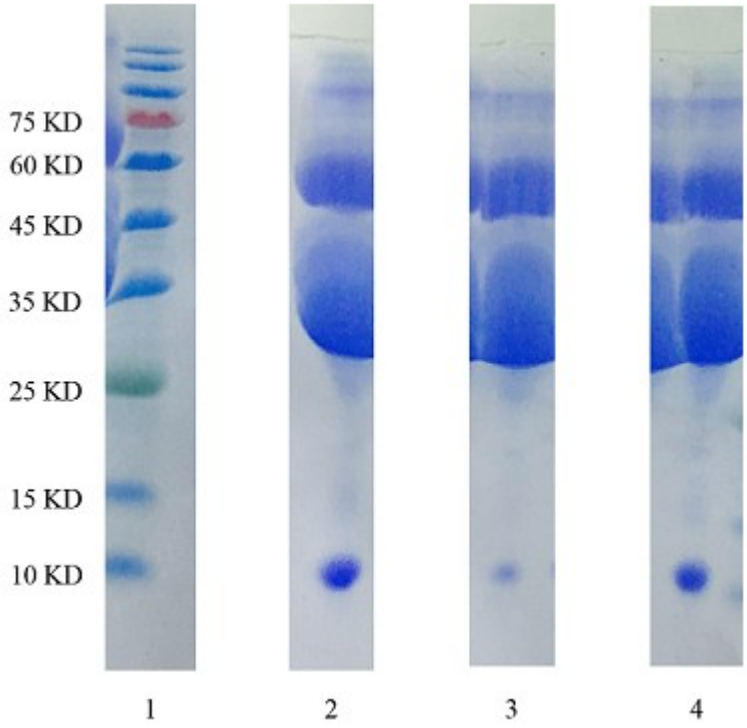

Fig. S9 The results of SDS-PAGE analysis for the separation of Lys from practical sample. Lane 1, protein molecular weight marker; Lane 2, 10-fold diluted chicken egg white; Lane 3, 10-fold diluted chicken egg white after adsorption by Fe_3O_4@VTEO@IL-MIPs; Lane 4, 10-fold diluted chicken egg white after adsorption by Fe_3O_4@VTEO@IL-NIPs.

The structures of the protein could be described by the circular dichroism spectra (CD spectra), which can further evaluate the conformational changes of Lys in the adsorption process by comparing the CD spectra before and after the elution. The magnetic Fe_3O_4@VTEO@IL-MIPs were eluted by SDS-HAc (2% W/V: 2% V/V) solution. As presented in Fig. S10, all the curves show similar shape and characteristic peak at 208 nm and 222 nm, which suggests that the secondary structures of Lys had no change after adsorption and elution.

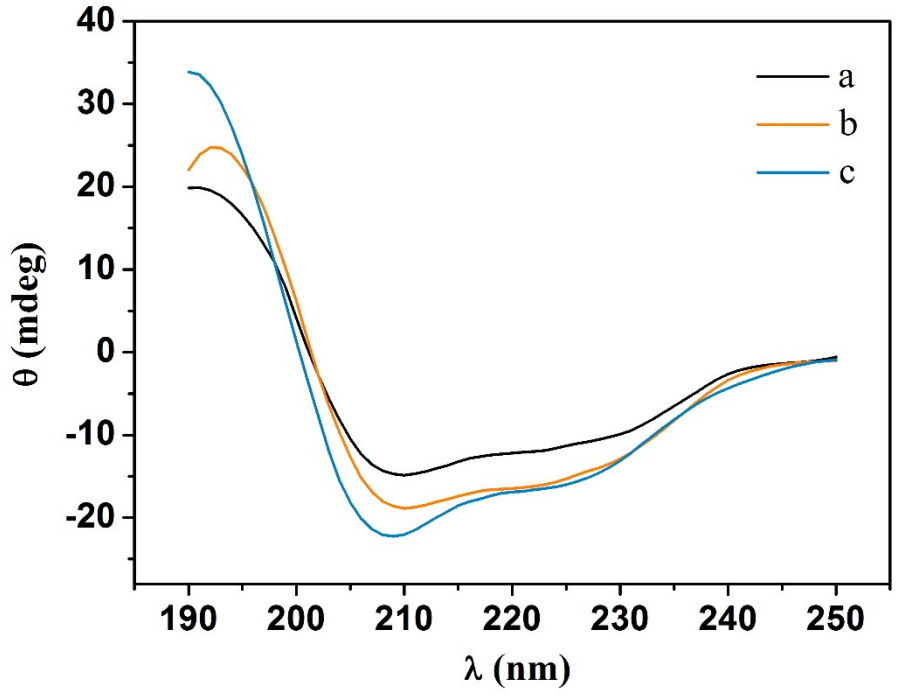

Fig. S10 The CD spectra of Lys in buffer buffer solution (pH = 7.1) before adsorption (a), the supernatant after adsorption (b); in the SDS-HAc (2% W/V: 2% V/V) solution eluted from Fe_3O_4@VTEO@IL-MIPs (c).

In addition, as illustrated in Fig. S11, UV-visible spectra of Lys in buffer solution (pH = 7.1) before adsorption (a), the supernatant after adsorption by Fe_3O_4@VTEO@IL-MIPs (b), Fe_3O_4@VTEO@IL-NIPs (c) and SDS-HAc (2% W/V: 2% V/V) solution eluted from Fe_3O_4@VTEO@IL-MIPs (d) have similar shape and characteristic peak at 280 nm. The result proves the structures of Lys doesn't be changed too much during adsorption.

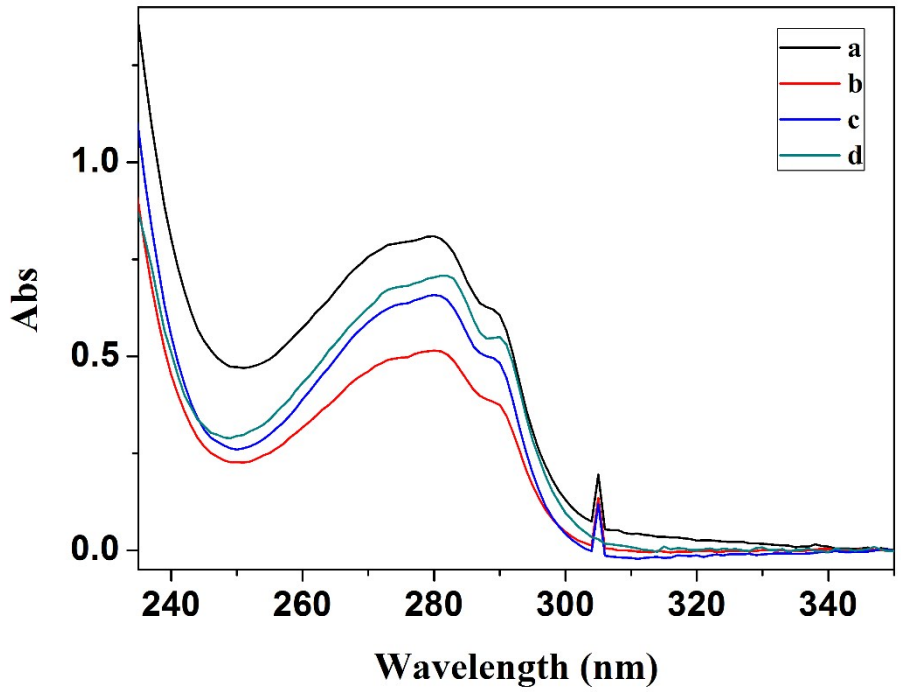

Fig. S11 The UV-visible spectra of Lys in buffer solution (pH = 7.1) before adsorption (a), the supernatant after adsorption by Fe_3O_4@VTEO@IL-MIPs (b); the supernatant after adsorption by Fe_3O_4@VTEO@IL-NIPs (c); in the SDS-HAc (2% W/V: 2% V/V) solution eluted from Fe_3O_4@VTEO@IL-MIPs (d)

References

1 M. Zhang, Y. Wang, X. Jia, M. He, M. Xu, S. Yang, C. Zhang, *Talanta*, 2014, **120**, 376-385.

2 J. Ashley, K. Wu, M. F. Hansen, M. S. Schmidt, A. Boisen and Y. Sun, *Anal. Chem*., 2017, **89**, 11484-11490.

3 C, Zhang. Y, Wang. J, Guo. Y, Liu and Y, Zhou, RSC Adv., 2015, **5**, 106197-106205.